Nano Biomed Eng
2019, 11(3): 313-319. doi: 10.5101/nbe.v11i3.p313-319.

Research Article

Preparation of Aluminum Oxide Nanoparticles by Laser Ablation and a Study of Their Applications as Antibacterial and Wounds Healing Agent

Kareem Hussein Jwad[1], Tahreer Hadi Saleh[2], Buthenia Abd-Alhamza[3]

[1]University of Technology, Departments of medical engineering, Iraq.
[2]Mustansyria University, College of Science, Biology department, Iraq.
[3]University of Technology, Departments of Applied Sciences-Division Biotechnology, Iraq.

Corresponding author. E-mail: karimuot@yahoo.com

Received: Jul. 30, 2019; **Accepted:** Sep. 10, 2019; **Published:** Sep. 19, 2019.

Citation: Kareem Hussein Jwad, Tahreer Hadi Saleh, and Buthenia Abd-Alhamza, Preparation of Aluminum Oxide Nanoparticles by Laser Ablation and a Study of Their Applications as Antibacterial and Wounds Healing Agent. *Nano Biomed. Eng.*, 2019, 11(3): 313-319.
DOI: 10.5101/nbe.v11i3.p313-319.

Abstract

Aluminum oxide nanoparticles were prepared and characterized with a wide variety of applications. This study aimed at the preparation of AlO_2 nanoparticles by the liquid particles treated with laser (1064 nm), immersed in deionized water at varied laser energy (350 J/cm^2) and diverse numbers of 300 pulse. For antimicrobial, antioxidants, animal's model, the prepared nanoparticles were confirmed by using ultraviolet–visible spectroscopy (UV-Vis), X-ray diffraction (XRD) and scanning electronic microscope (SEM). The antimicrobial activity of synthesized Al_2O_3 nanoparticles was tested using well diffusion method against three types of bacteria: *Escherichia coli*, *Pseudomonas aeruginosa* and *Staphylococcus aureus*. The best concentration of aluminum oxide nanoparticles was 100 mg/mL, which exhibited a higher antibacterial activity against both gram-negative and -positive bacteria. In addition, the results showed that the gram-negative bacteria were more resistible than gram-positive bacteria. The results also indicated that the aluminum oxide nanoparticles possessed antioxidant effects, as investigated by DPPH method. Finally, the wound healing activity of the aluminum oxide nanoparticles was investigated, and the results showed that the aluminum oxide nanoparticles stimulated the wound healing activity by using animal's model. The results presented in this study demonstrated that the aluminum oxide nanoparticles had biomedical applications could be applied in biomedical uses in the future.

Keywords: Aluminum oxide nanoparticles; Antimicrobial; Antioxidants; Wound healing

Introduction

The past years have witnessed the development of nano-oxide particles on a large scale. Nano-oxide particles are used in several applications including medical science, semiconductors, batteries, sensors, capacitors and catalysts [1, 2]. Among all Al_2O_3 is generally mentioned to exist in corundum that has numerous phases like Y, β, **θ**, α and δ; α-alumina phase is the most stable thermodynamically stage. Alumina has several properties such as high hardness, high stability, high insulation, and transparency [3].

Al_2O_3 is commonly used in the surface protective coating, catalyst, insulator, and composite materials [4]. Al_2O_3 nanoparticles (NPs) can be produced via many techniques involving, ball milling, sol-gel, sputtering hydrothermal, pyrolysis, and laser ablation [5-7]. Among them, the laser ablation is a extensively used technique for the production of NPs, since it can be synthesized in void or liquid and gas. This method offers some advantages such as rapid and high purity process compared with other methods [8]. Moreover, synthesizing NPs through laser ablation via liquid is simpler than the by gas atmosphere [9, 10]. The present study attempted to prepare AlO_2 NPs by using liquid particles treated with laser technology (1064 nm) and energy (350 MJ), and to study their medical application as antibacterial and stimulation of wound healing.

Experimental

Preparation of colloidal Al_2O_3 NPs

Al_2O_3 disk target (99.7%) in distilled water was irradiated with pulse Nd: YAG laser system (at 1064 nm, pulse duration = 9 ns, repetition rate 1 Hz) with maximum energy of 300 MJ per pulse. This setting was used for Al_2O_3 NPs perpetration with an ablation time of 30 min (Fig. 1).

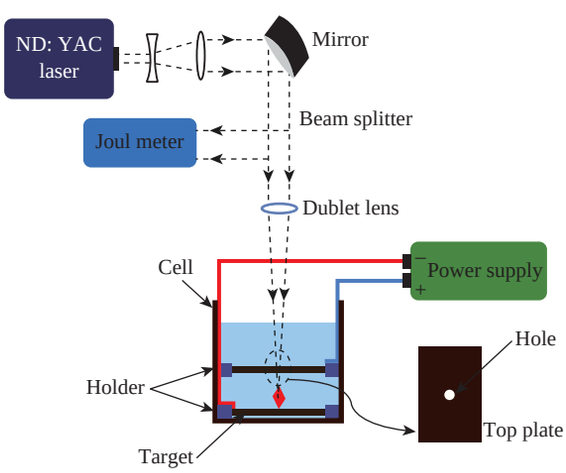

Fig. 1 Al_2O_3 NPs perpetration with a laser ablation.

Ultraviolet–visible spectroscopy (UV-Vis)

UV-Vis spectrophotometer model SP-3000 Plus, OPTIMA was used to investigate the optical absorption spectra of colloids within the spectral range of 200-800 nm for AL_2O_3 NPs.

X-ray diffraction (XRD)

XRD pattern was obtained by using XRD 6000 Shimadzu Japan, Cu-Kα radiation source at 2θ angel = (20-80) degree. XRD is a technique used for phase identification of a material. The grains size was calculated from the width of the XRD peaks, using the Scherrer formula [11]:

$$D = 0.94\lambda/\beta \cos\theta, \quad (1)$$

where λ is the X-ray wavelength (1.54060 Å), and β is the full-width.

Scanning electron microscopy

SEM assay surface characteristics were evaluated by scanning electron microscope (SEM), Stereoscan 360, Cambridge at 10 kV, and θ is the diffraction angle.

Antibacterial activity assay

The antibacterial activity of aluminum oxide NPs was performed based on the work by Jabir and coworkers [12], against some pathogenic bacteria such as *Escherichia coli* (*E. coli*), *Pseudomonas aeruginosa* (*P. aeruginosa*) and *Staphylococcus aureus* (*S. aureus*) by well diffusion method. Bacterial suspension existed on Muller Hinton agar; then the plates were punctured with a 6 mm well, using sterile tip. Aluminum oxide NPs at various concentrations of 25, 50, 75 and 100 mg/mL were poured into the well and incubated at 37 °C for 24 h. The inhibition zone was measured. The experiment was conducted for 3 replicates [13].

DPPH radical scavenging assay

Antioxidant activity was estimated by 2, 2-diphenyl-1-picryl-hydrazyl-hydrate assay according to the method as described by Swarnkar et al. [14] with some modifications. Every tested compound (10 µL) was mixed with absolute ethanol (490 µL), and the quantity was completed to 1 mL by addition of DPPH solution, incubated at room temperature for 15 min. The left-over amount of 2,2-diphenyl-1-picryl-hydrazyl-hydrate was determined based on the decline in absorbance at 517 nm. The scavenging percentage was calculated by equation:

$$\text{Scavenging\%} = [(\text{Ab control} \mid \text{Ab sample})/\text{Ab control}] \times 100\%.$$

Stimulation of wound healing by aluminum oxide nanoparticles

The role of aluminum oxide NPs inside the living body in the healing of wounds was studied. The wound was cut as of 2 cm^2 on the surface (dorsal) of the body of the mouse and was then treated with oxide aluminum NPs. The control group was treated using

phosphate-buffered saline (PBS) solution, as obtained from the Center of Biotechnology Research, Nahrain University. At 8 weeks of age, the experimental mice (20 to 25 g each) were randomly divided into two groups of three mice per group (control and treatment).

Statistical analysis

The data are presented as mean ± SEM. Statistical analysis was done using unpaired t-test with GraphPad Prism 6**.** Differences were considered as being significant at $p < 0.05$.

Results and Discussion

Characterization

The optical absorbance of aluminum oxide NPs obtained from the laser energy of 5 J is summarized in Fig. 2, with the highest absorption peak recorded at 220 nm. The concentration of aluminum oxide NPs was high, and the size of oxide aluminum NPs depended on the increase of laser energy. The NP colloids produced energy of 5 J, showing little difference in their optical absorption characteristics. XRD analysis for Al_2O_3 NPs is presented in Fig. 3 which shows 6 distinct diffraction peaks at 2θ, including 33.30, 38.56, 44.48, 55.58, 61.20 and 66.30 which corresponded to the 220, 222, 400, 311,511 and 440 of the cubic face-centered. On the other hand, the SEM image also showed spherical shape for Al_2O_3 NPs (Fig. 4).

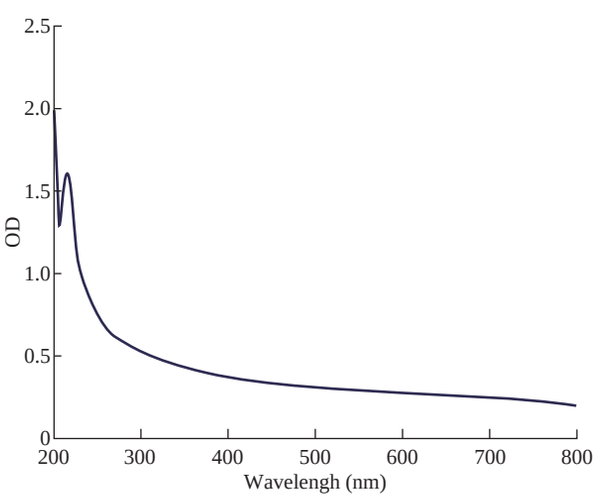

Fig. 2 UV-Vis absorbance spectra of AL_2O_3 NPs prepared by laser ablation in DIW at 5 J.

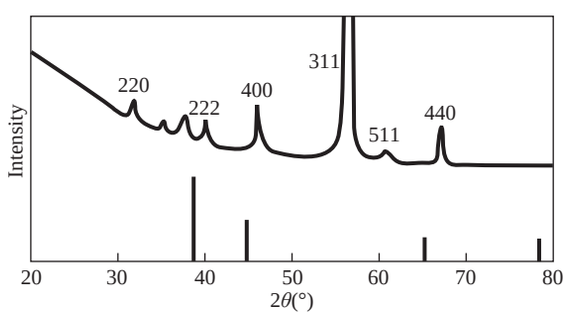

Fig. 3 XRD of AL_2O_3 NPs prepared by laser ablation at 5 J.

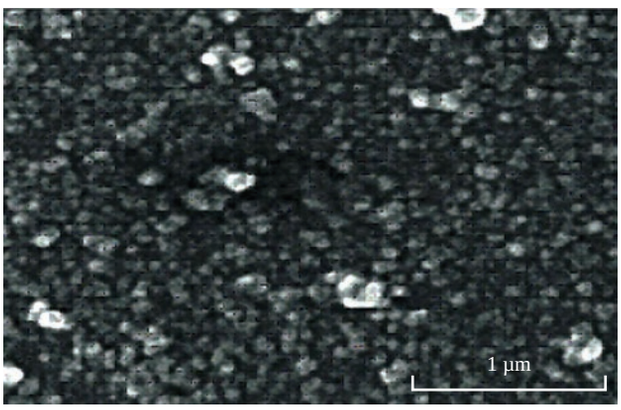

Fig. 4 SEM of AL_2O_3 NPs prepared by laser ablation in DIW at 5 J.

In vitro study of antibacterial activity

The antibacterial activity of Al_2O_3 NPs was examined against three types of pathogenic bacteria, using well diffusion method (Fig. 5). The two gram-negative bacteria were *E. coli* and *P. aeruginosa*; the one gram-positive bacterium was *S. aureus*. Aluminum oxide NPs were used at different concentrations of 25, 50, 75 and 100 mg/mL, and the inhibition zone was measured. The results showed the inhibition zone increased with the increasing of concentration. The highest effect of antibacterial activity against *S. aureus* was measured to be 25.55 mm, and the inhibition activity was measured to be 20.56 mm and 19.33 mm against *E. coli* and *P. aeruginosa*, respectively (Table 1).

DPPH assay radical scavenging assay

The percentage of scavenging activity is shown in Fig. 6, Al_2O_3 NPs with 100 µg/mL concentration showed an antioxidant activity of 78.3%.

Wound healing activity by AL_2O_3 nanoparticles

Wound healing activity of the prepared Al_2O_3 NPs was tested in three male mice by excision wound model. The results showed high efficiency of Al_2O_3 NPs in wound treatment compared with the control, i.e. the non-treated group. The duration of the treatment lasted for three weeks. In the first week, the wound treated with NPs revealed distinguished wound closure. In the second week, size of the would was shown to be smaller. In the last week, the aluminum oxide NPs

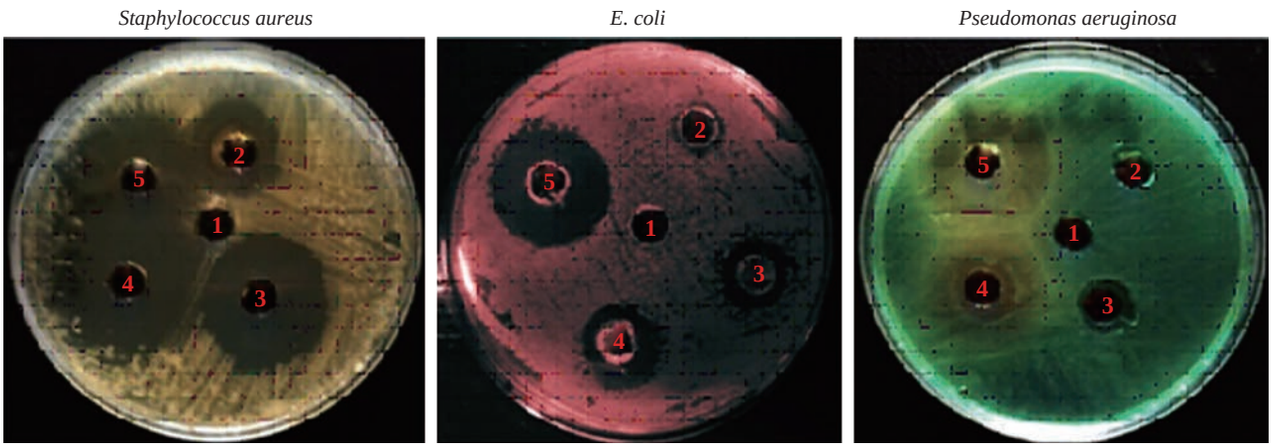

Fig. 5 Antibacterial effect of Al_2O_3 NPs against gram-positive bacterium *S. aureus* and gram-negative bacteria *E. coli* and *P. aeruginosa*.

Table 1 Antibacterial activity of Al_2O_3 NPs prepared by laser ablation at 5 J

Microorganism	Aluminum oxide NPs concentration (µg/mL)				
	25 %	50%	75%	100%	Control D.W
E. coli	9.56 mm	12.55 mm	15.56 mm	20.56 mm	--
S. aureas	15.56 mm	15.33 mm	20.33 mm	25.55 mm	--
P. aeruginasa	6 mm	7.55 mm	18.50 mm	19.33 mm	--

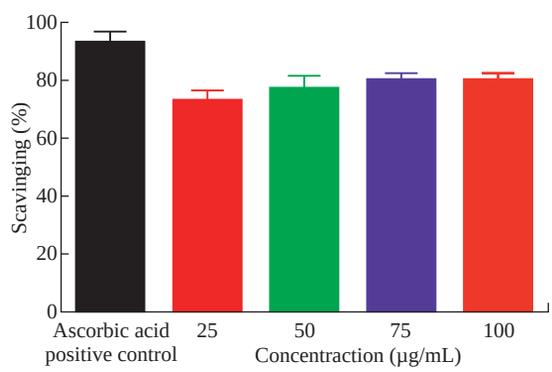

Fig. 6 Antioxidant activity of AL_2O_3 NPs.

showed the highest effect of closure, whereas the control group showed lower level of closure (Fig. 7).

The NP colloids produced by energy of 5 J showed little difference in their optical absorption characteristics, which may be attributed to morphological similarities. The increase of laser energy increased the NPs' size. Absorption decreased continuously above 220 nm, and the optical absorption edges shifted slightly towards longer wavelength (red shift). This shift resulted from the increase in particle size [15]. The structural properties of XRD analysis for Al_2O_3 NPs showed six distinct diffraction peaks at 2θ = 33.30, 38.56, 44.48, 55.58, 61.20 and 66.30, which correspond to the 220, 222, 400, 311,511 and 440 of the cubic face-centered, according to Al_2O_3 NPs (JCPDS-ICDD) Card Nos. 85-1327 and 29-0063, respectively. It was seen from the XRD spectra that all particles were obtained from the laser ablation with laser energy at 5 J. This led to the conclusion that the particle concentration, suspended in deionized water, obtained from laser energy of 5 J was higher. The grain size (D) values of the synthesized sample were calculated by Scherer's equation using Equation (1). However, SEM assay was analyzed by Image J and software was employed to visualize the shape of compounds. Image of SEM exhibited relatively spherical shape of Al_2O_3 NPs with diameter in the range of 10 to 60 nm (Fig. 4). However, the total particle size of Al_2O_3 NPs was of about 200 particles, which was due to more collisions between the atoms as a result of the energy product by the laser. In this study, the antimicrobial activity Al_2O_3 NPs with different concentrations was investigated. The highest effect against pathogenic bacterial isolates reached 100 mg/mL, while, the lower effect was at the concentration of 25 mg/mL. Variable results were shown in the effectiveness of concentrations of 50 and 75 mg/mL (Fig. 5 and Table 1). Al_2O_3 NPs revealed higher activity against gram-positive bacteria compared with gram-negative bacteria. The difference in the responses of both gram-positive and -negative

Fig. 7 In-vivo effect of Al_2O_3 NPs as wound healing agent.

bacteria against the same prepared Al_2O_3 NPs resulted from the difference in the structure of cell wall between the bacteria. The gram-negative bacteria had an outer membrane containing lipopolysaccharide structure which makes the cell wall more resistant to the lipophilic solutes, while the gram-positive bacteria had an outer thick layer of peptidoglycan making it more susceptible to these NPs [16, 17]. The metal oxide had an active role in the inhibition of growth of bacteria by the generation of reactive oxygen species that could induce oxidative stress in the bacterial cells, Moreover, the presence of aluminum metal ions could promote Fenton reactions which led to reactive oxygen species (ROS) generation being enhanced [18, 19]. There have been many studies promoting the antibacterial activity of some metal oxide NPs, one of which showed that the effect of these NPs could be antibacterial, due to their unique physical and chemical characteristics and large surface area to volume ratio making them enhance the antibacterial activity for some agents [20]. Other studies have revealed that the metal oxide NPs have a different antibacterial mechanisms which involve the release of ROS, damaging cellular structures of bacteria, disruption of bacterial membranes and cell wall, and the inhibition of enzyme activity and DNA synthesis [21, 22].

Iron oxide NPs can kill bacteria by destruction of their biofilms [23, 24]. As observed in this study, the antibacterial activity of alumina NPs due to the release of metal ions played a major role in NPs' toxicity. It was shown that alumina NPs had a positive charge; therefore, they were strongly attached to the surface of bacteria that had a negative charge. Bala et al. [25] investigated the antibacterial effect of alumina NPs towards *E. coli*, *P. aeruginosa*, and *Bacillus subtilis* by using SEM. The SEM image showed the interaction between alumina NPs and bacterial cells, clearly indicating the change in cell morphology and the aggregated particles on the cell wall. The alumina-interacted cells showed distorted cell morphology, indicating the distortion of bacterial cells [26]. Also, Murdock et al. [27] observed that the behavior of alumina NPs was also influenced by particle size, shape and charge of surface. NPs tend to agglomerate in hard water and seawater because NPs interact with organic matters that are present in water; agglomeration of these nanoparticles is also influenced by the salinity and the pH of water.

DPPH has stable free radicals associated with spare electron. Free radicals of DPPH delocalize over the entire molecule, barring its dimerization. The delocalization of electron also gives rise to the deep violet color, characterized by an absorption band of 517 nm in ethanol solution. When the solution of DPPH is mixed with a substrate that can donate a hydrogen atom, this will give rise to the reduced form with the loss of violet to yellow [28]. The percentage of scavenging activity is shown in Fig. 6, Al_2O_3 NPs at the concentration of 100 μg/mL showed an antioxidant activity of 78.3%. It is interesting to find that our results agreed with results of other literatures that confirmed the role of AL_2O_3 NPs as ROS scavenger. It has been revealed that a major problem with diabetic patients is the delay of wound healing. This is because of the increase in oxidative stress and the decrease

in antioxidant content, which results in inflammation and production of large amounts of ROS, leading to disruption of wound healing. These harmful products can be repaired by using some groups of metal oxide NPs such as alumina, CeO_2 and Y_2O_3 that have essential role in diabetic wound healing mediated by ROS scavenging potentials and lead to therapy of wound healing in diabetic patients [29, 30].

Wound healing activity for Al_2O_3 NPs was shown in the treated mice by excision wound model compared with the control during treatment stages (Fig. 7). Oxidative stress was a major contributor to delayed wound healing and produced large amounts of ROS by increasing inflammation [31]. Wound healing is a complex sequence, including cellular and molecular process, such as inflammation, angiogenesis, cell migration, provisional matrix synthesis, collagen deposition and re-epithelization. The healing process requires a sophisticated interaction among inflammatory cells, biochemical mediators, extracellular matrix molecules and micro environmental cell populations, all of which are stimulated by a number of mitogens and chemotactic factors. Meanwhile, healing impairment is characterized by delayed cellular infiltration and granulation tissue formation, reduced angiogenesis, decreased collagen, and organization; all of these signs have been shown in the mice untreated with NPs. The mechanism of this alteration is thought to result from production of high levels of reactive oxygen species and increased levels of apoptosis, which in turn impair keratinocyte endothelial cells, fibroblast and collagen metabolism [32]. Iron oxide NPs are known to be of small size, large surface area and high susceptibility attachments with carbon nanotubes that can easily penetrate the hair follicle, resulting in increased and regenerated hair growth with mice treated by NPs [33].

Conclusions

In this study, preparation of aluminum oxide NPs was conducted using laser technique. Some biomedical applications of the prepared NPs were studied. The results presented in this study demonstrated that the aluminum oxide NPs had antimicrobial, antioxidant and wound healing activities. Hence, they could be used in the field of biomedical applications.

Conflict of Interests

The authors of this work assume full responsibility for the content of this paper, and hence declare no conflict of interest.

References

[1] W. Ueda, M.Sadakane, and H. Ogihara, Nano-structuring of complex metal oxides for catalytic oxidation. *Catal Tod*, 2008, 132(1-4): 2-8.

[2] P.D. Pria, Evolution and new application of the alumina ceramics in joint replacement. *Europ J Ortho Surg Traum*, 2007, 17(3): 253-256.

[3] L.D. Hart, *Alumina chemicals: Science and technology handbook*. Ameri Cera Soci Colum, Ohio, USA, 1990.

[4] A. Laachachi, M. Ferriol, M. Cochez, et al., A comparison of the role of boehmite (AlOOH) and alumina (Al_2O_3) in the thermal stability and flammability of poly (methyl methacrylate). *Polym Degrad Stab*, 2009, 94(9):1373-1378.

[5] C.B. Reid, J.S. Forrester, H.J. Goodshaw, et al., A study in the mechanical milling of alumina powder. *Cera Internat*, 2008, 34(6): 1551-1556.

[6] D.H. Trinh, M. Ottosson, M. Collin, et al., Nanocomposite Al_2O3-ZrO_2 thin films grown by reactive dual radio-frequency magnetron sputtering, *Thin Solid Film*, 2008, 516(15): 4977-4982.

[7] K. Yatsui, T. Yukawa, C. Grigoriu, et al., Synthesis of ultrafine γ-Al2O3 powders by pulsed laser ablation. *J Nanop Rese*, 2000, 2(1): 75-83.

[8] A. Kruusing, *Handbook of liquids-assisted laser proces*. Elsev, 2008.

[9] I.L. Liu, P. Shen, and S.Y Chen, H+- and Al_2+-codoped Al_2O3 nanoparticles with spinel-type related structures by pulsed laser ablation in water. *J Phys Chem C*. 2010, 114(17): 7751-7757.

[10] B. Kumar, R.K. Thareja, Synthesis of nanoparticles in laser ablation of aluminum in liquid. *J Appl Phys*, 2010, 108(6): 064906-064906-6.

[11] W.K.A. Kadhim, U.M. Nayef, and M.S. Jabir, Polyethylene glycol-functionalized magnetic (Fe3O4) nanoparticles: A good method for a successful antibacterial therapeutic agent via damage DNA molecule. *Surface Review and Letters*, 2019: 1950079.

[12] M.S. Jabir, U.M. Nayef, K.H. Jawad, et al., Porous silicon nanoparticles prepared via an improved method: a developing strategy for a successful antimicrobial agent against Escherichia coli and Staphylococcus aureus. *IOP Conference Series: Materials Science and Engineering*, 2018, 454: 012077.

[13] G.P. Dufour, C.M. Loonis, and O. Dangles, Quantitative kinetic analysis of hydrogen transfer reactions from dietary polyphenols to the DPPH radical. *J Agric Food Chem*, 2003, 51(3): 615-622.

[14] R.K. Swarnkar, S.C. Singh, and R. Gopal, Effect of aging on copper nanoparticles synthesized by pulsed laser ablation in water: Structural and optical characterizations. *Bull Mate Scie*, 2011, 34(7): 1363-1369.

[15] M.T. Cabeen, C. Wanger, Bacterial cell shape. *Nat Rev Microbial*, 2005, 3(8): 601-610.

[16] S.A. Ibraheem, H.A. Kadhem, S.A. Hadeethi, et al., Effects of silver nanoparticles on nosocomial Pseudomonas aeruginosa strains–an alternative approach for antimicrobial therapy. *Romanlan Biotechnological Letters*, 2019, 24: 286-293.

[17] M.S. Jabir, G.M. Sulaiman, Z.J. Taqi, et al., Iraqi propolis increases degradation of IL-1β and NLRC4 by autophagy following Pseudomonas aeruginosa infection. *Microbes and Infection*, 2018, 20: 89-100.

[18] M.S. Jabir, U.M. Nayef, and W.K.A. Kadhim,

Polyethylene glycol-functionalized magnetic (Fe_3O_4) nanoparticles: A novel DNA-mediated antibacterial agent. Nano Biomedicine and Engineering, 2019, 11(1): 18-27.

[19] K.S. Khashan, M.S. Jabir, and F.A. Abdulameer, Carbon nanoparticles decorated with cupric oxide Nanoparticles prepared by laser ablation in liquid as an antibacterial therapeutic agent. *Materials Research Express*, 2018, 5: 035003.

[20] W.K.A. Kadhim, U.M. Nayef, and M.S. Jabir, Polyethylene glycol-functionalized magnetic (Fe_3O_4) nanoparticles: A good method for a successful antibacterial therapeutic agent via damage DNA molecule. *Surface Review and Letters*, 2019: 1950079.

[21] K.S. Khashan, M.S. Jabir, and F.A. Abdulameer, Preparation and characterization of copper oxide nanoparticles decorated carbon nanoparticles using laser ablation in liquid. *Journal of Physics: Conference Series*, 2018, 1003: 012100.

[22] K.S. Khashan, M.S. Jabir, and F.A. Abdulameer, Carbon Nanoparticles prepared by laser ablation in liquid environment. *Surface Review and Letters*, 2019: 1950078.

[23] J.W. Mashayekhi, H.B. Xing, Bacterial toxicity comparision between nano- and micro- scale oxide particles. *Enviro Pollu*, 2009, 157(5): 1619-1625.

[24] B.T, Armstrong, G.F. Laffir, and R.T. Thornton, Titania-silver and alumina-silver composite nanoparticles: novel, versatile synthesis, reaction mechanism and potential antimicrobial application. *J Coll Interface Scien*, 2011, 356(2): 395-403.

[25] M.S. Jabir, A.A Taha, and U.I Sahib, Linalool loaded on glutathione-modified gold nanoparticles: a drug delivery system for a successful antimicrobial therapy. *Artificial Cells, Nanomedicine, and Biotechnology*, 2018, 46: 345-355.

[26] S.H. Ali, G.M. Sulaiman, M.F. Al-Halbosiy, et al., Fabrication of hesperidin nanoparticles loaded by poly lactic co-Glycolic acid for improved therapeutic efficiency and cytotoxicity. *Artificial Cells, Nanomedicine, and Biotechnology*, 2019, 47: 378-394.

[27] M.S. Jabir, A.A. Taha, U.I. Sahib, et al., Novel of nano delivery system for Linalool loaded on gold nanoparticles conjugated with CALNN peptide for application in drug uptake and induction of cell death on breast cancer cell line. *Materials Science and Engineering*, 2018, 94: 949-964.

[28] M.M. Kumar, H.K.Tripathi, Diabetic delayed wound healing and the role of silver nanoparticles. *Dig J Nanomater Bios*, 2008, 3(2): 49-54.

[29] D.B. Warheit, Nanoparticles: health impacts? *Mater Tod*, 2004, 7(2): 32-35.

[30] C. Roberta, V. Vincenzo, L. Laura, et al., Nanoscale particles therapies for wound healing. *Nanomedicine*, 2010, 5(4): 641-656.

[31] G.M. Sulaiman, M.S. Jabir, and A.H. Hameed, Nanoscale modification of chrysin for improved of therapeutic efficiency and cytotoxicity. *Artificial Cells, Nanomedicine, and Biotechnology*, 2019, 46: 708-720.

[32] J. Yup, W.C. Dong, Functionalization of carbon nanotubes. *Carbon nanotubes - polymer nanocomposites*. InTech, Rijeka, Croatia, 2011: 91-110.

[33] K.H. Jawad, N.N. Hseean, and B.A. Hasoon, Study and synthesis of Fe_3O_4 nanoparticles prepared by laser ablation and Its biomedical application. *Journal of Engineering and Applied Sciences*, 2018, 13: 10633-10638.